Carpathian Journal of Earth and Environmental Sciences, August 2020, Vol. 15, No. 2, p. 429 – 441; Doi:10.26471/cjees/2020/015/142

A COMPARISON OF TWO BEDROCK RIVER STREAM-POWER EROSION MODELS: A CASE STUDY OF THE RIVER PROFILE OF THE GYIRONG WATERSHED IN THE MIDDLE HIMALAYAN OROGEN

Lu CHEN[1,2], Aike KAN[3,*], Guiping DENG[3], Jianxiong QIN[4], Qinghong RAN[1] & Jun HE[5]

[1]Institute of Humanity Resources in Western China, Chengdu Normal University, Chengdu 611130, China
[2]Institute of Science & Technology Information of Tibet Autonomous Region, Lhasa 850001, China
[3]College of Tourism and Urban-Rural Planning, Chengdu University of Technology, Chengdu 610059, China,
**Coresponding author email kanaike@cdut.edu.cn, 13408572118*
[4]College of Historical Culture and Tourism, Southwest Minzu University, Chengdu 610059, China
[5]Shannan Branch of Hydrology and Water Resources Survey Bureau of Tibet Autonomous Region, Shannan 856000, China

Abstract: The models for quantitative study of bedrock river are two typical representatives: the Distance-slope (DS) Model and the Area-slope (AS) Model. The AS model introduces the law of the matter conservation and builds a bridge between tectonic uplift and erosion. In recent decade, AS has been widely used in the longitudinal profile simulation of bedrock and alluvial rivers, but many applications have failed to carefully consider the mechanism, fitting effect, and applicability of the resulting models, resulting in unsatisfactory simulation results. In order to verify the channel profile analysis capability of the two models, the study compared the theoretical basis and the applications of channel fitting and knickpoint identification made in the Gyirong Watershed in the middle Himalayan Orogen. It is believed that if the river meets the equilibrium condition, both models reflect the law of the matter conservation, instead of being limited to the AS. The results show that, for rivers with different equilibrium status, the two have different numerical responses on 7 bedrock rivers. The AS model has a comparative advantage in river channels with a higher degree of equilibrium, while the DS model is more suitable for longer rivers in a disequilibrium state. Finally, we applied DS model to the Gyirong Zangbo River in order to analyze the numerical characteristics of the knickzone parameters. It is found that the distribution of concave-convex intersection on the profile corresponds to the variation of the fast and slow erosion rate. This characteristic reflects the interaction between the river erosion and sedimentation in the Gyirong Watershed and is sensitive to the formation processes of the differentiated climate patterns over the past 2 Ma

Keywords: Bedrock River; Stream-Power Erosion Models; river-fitting; knickpoint; Gyirong Watershed

1. INTRODUCTION

A bedrock river, which is a rock bound reach in the riverbed or riverbank (Whipple et al., 2013). Mountainous bedrock rivers generally develop in active collision zones (Brookfield, 2008; Kirby et al., 2003), passive continental margins (Bishop & Goldrick, 2000), and intracontinental tectonic zones (Formento-Trigilio & Pazzaglia, 1998; Flint, 1973). Since the 1950s, the mathematical and physical relationships of river terrain properties has been widely used in studies of large-scale regional landscape evolution due to land uplift or base-level changes (Vijith et al., 2017; Brookfield, 1998; Seever & Gornitz, 1983; Flint, 1973; Hack, 1957) and two empirical power models of the bedrock river stream-power erosion were established in the 1990s (Howard et al., 1994): the distance-slope model is based on the upstream distance and gradient (Goldrick & Bishop, 2007; Hack, 1973); and the area-slope model is based on the drainage area and the river gradient (Willgoose, 1994; Howard & Kerby, 1983). However, the two models have some common problems: the profile parameters (e.g. steepness and degree of convex-concave structure) of different reaches vary

significantly, profile scatter plots are usually not ideal; the spatial scale of the tectonic region corresponding to the validity of the model is unclear; and the models are based on the assumption of a river in equilibrium, but erosion and uplift are generally inconsistent in time and space, so absolute equilibrium is unrealistically ideal. Therefore, it is necessary to test the whole process from model theory to model application.

This study first compares the theoretical basis of the two models. Then in the Gyirong Watershed, which is a typical tectonically active region in the middle Himalayan Orogen, we compared the results of the DS and AS models with respect to their abilities to fit the river channels and identify the river knickpoints. Finally, we applied the results above to analyze the numerical characteristics over the trunk of Gyirong Watershed. This study provides theoretical and empirical research on two kinds of bedrock river stream-power erosion models for other scholars to understand and apply the models.

2. THEORETICAL BASIS OF THE MODELS

Equilibrium means that under the influence of internal and external forces such as climate, lithology, and structure, the river channel has been fully deformed and adjusted at an average erosion rate. As the downstream extent of the river grows, the river's elevation gradually decreases and the longitudinal profile becomes concave. The form of a concave equilibrium channel can be simulated by the power function of several topographic variables, including the elevation, the gradient, the river width, and the river discharge. In addition, the abrupt changes in longitudinal river profiles can be used to analyze the structural causes of the river landscape evolution due to uplift and erosion (Fig. 1).

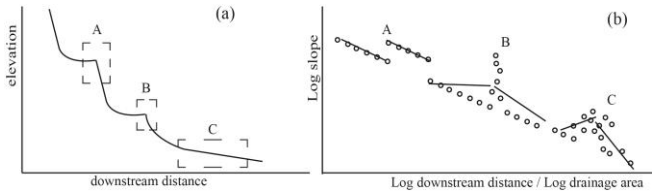

Figure 1 Schematic diagram of a hypothetical river profile with three types of crack section (a) corresponded to three types of knickpoint (b). Changes in lithology and corrosion resistance through A, the regression lines of the two sections are parallel, only the slopes are different. Unchanged in internal and external forces through B, the regression lines of both channels are not parallel, the slope is nearly symmetrical. Channel is disequilibria at C, the scatters are irregular. (redrawn from Goldrick & Bishop (2007) figure 6; copyright John Wiley and Sons Ltd and reproduced with permission)

2.1. DS Model

The DS model emphasizes the overall kinetic energy of the river, i.e., the longer the river, the greater the stream power. As the upstream distance (L) increases, the discharge (Q) increases exponentially (Hack, 1973) according to:

$$Q = lL^{\lambda} \tag{1}$$

where l and λ are constants. Each river has a gradient (S) a discharge (SQ) under the action of gravity, and an incision rate (I). In addition, the riverbed's bedrock interacts with the water flow, producing corrosion resistance (R). In equilibrium, the average rate of incision (I_{grade}) can be expressed by the discharge, the gradient, and the resistance (Goldrick &Bishop, 2007):

$$I_{grade} = \frac{iSQ}{R} \tag{2}$$

where i describes the proportion of incision accommodated by the river's kinetic energy, it is also a function of the stream hydraulic geometry. By substituting Equation (1) into Equation (2), the DS model is obtained:

$$S = kL^{-\lambda} \text{ or } \ln S = \ln k - \lambda \ln L \tag{3}$$

Where

$$k = \frac{RI_{grade}}{il}$$

Particularly, if λ=1,

$$S = \frac{dH}{dL} = -kL^{-1} \tag{4}$$

and H is the elevation. By integrating the two sides of Equation (4), we obtained the following equation:

$$H = -k \ln L + c \tag{5}$$

This equation is Hack's SL equation, which is a special form of the DS model. Equation 3 is the general form of the DS model. Similar to Hack's interpretation, k and λ reflect the changes in R and I_{grade} shown in Equation 3, which are indicators of the river's properties (Table 1).

2.2. AS Model

If all of the water channels are in the same state, there is a power relationship between the discharge (Q) and the upstream drainage area (A):

$$Q = k_q A^c \tag{6}$$

where k_q is a dimensionless coefficient, and c is a

Table 1 Indication of the nature of river profile based on k-λ

	Mode 1	***Mode 2***
For $k=\frac{RI_{grade}}{il}$	*If I_{qrade} is constant, R is variable when the river channel is in equilibrium and the average erosion rate is stable.*	*If R is constant, I_{qrade} is variable when the lithology is consistent, but the river is in disequilibrium or the state is unknown.*
Meanings of changes in K-λ	*R increases as K increases, indicating that if the bedrock has strong corrosion resistance and the river channel has a small degree of concaveness, λ should decrease.*	*I_{qrade} increases as K increases, indicating that if the average erosion rate and the degree of concaveness are large, λ should increase.*
	If K decreases, R will decrease, indicating that if the bedrock has weak corrosion resistance and the river channel has a large degree of concaveness, λ should increase.	*I_{grade} decreases as K decreases, indicating that if the average erosion rate and the degree of concaveness are small, λ should decrease.*

positive constant close to 1. The bedrock channel erosion rate (E) is a function of the shear stress incision (τ_b) (Howard et al., 1994; Howard & Kerby, 1983):

$$E = k_b \tau_b^a \tag{7}$$

where k_b is a dimensional correlation coefficient determined by the interaction between the erosion process, the resistance of the rock, and the sediment flux of the riverbed. a is a positive constant and $a \in [1, 5/2]$, indicating that the degree of shear stress incision ranges from slight linear incision to strong abrasion (Anderson et al., 2015). In hydraulics, the shear stress of the riverbed (τ_b), the discharge (Q), the gradient (S), and the channel width (W) combine to create the following relationship:

$$\tau_b = \rho C_f^{1/3} (gSQ/W)^{2/3} \tag{8}$$

where ρ is the water density, C_f is the dimensionless friction coefficient, and g is the gravitational acceleration. These variables represent resistance factors to shear along the rocks on the riverbeds and riverbanks. In addition, as the river extends downstream, the channel width takes the form

$$W = k_w Q^b \tag{9}$$

where k_w is the dimension coefficient, and b is a positive constant. Combining equations 6-9 results in the well-known shear-stress incision function

$$E = K A^m S^n \tag{10}$$

Where

$$K = k_q^{2a(1-b)/3} k_b k_w^{-2a/3} \rho^a C_f^{a/3} g^{2a/3} \tag{10-1}$$

$$m = 2ac(1-b)/3 \tag{10-2}$$

$$n = 2a/3 \tag{10-3}$$

After rearranging the function, the classic expression of the AS model can be rewritten as

$$S = k_s A^{-\theta} \text{ or } \ln S = \ln k_s - \theta \ln A \tag{11}$$

Where

$$k_s = (E/K)^{1/n} \tag{11-1}$$

$$\theta = m/n \tag{11-2}$$

Howard et al., (1994) incorporated the law of matter conservation into the AS model, and proposed that the average erosion rate and the average uplift rate of the rock are equal relative to the base level over time. Thus, the river elevation can be expressed as a function of time. Whipple et al., (2013) quantitatively determined that the river required more than 100 ka to reach an equilibrium state. The mathematical expression is as follows:

$$dz/dt = U - E \tag{12}$$

where z is the elevation of any point in the river, t is the time, U is the average uplift rate of the rock, and E is the average erosion rate of the river. If the river is in equilibrium, $dz/dt=0$, $U=E$, and Equation 11-1 is applicable, then

$$k_s = (U/K)^{1/n} = (E/K)^{1/n} \tag{13}$$

Bedrock uplift and river erosion control the changes in the channel elevation; k_s is the river steepness index, and θ is the concave index affecting the fluctuation of the river channels. Both parameters affect the model's fitting ability.

The direct goal of the DS and AS models is to simulate the form and structure of the river and to indicate the potential location of the knickpoint. Both models are based on the idea that the water's erosive force is derived from the kinetic energy of the river. Nevertheless, the factors determining the erosive force are different, resulting in different model variables. The AS model is based on the fact that the physical processes involved in modern river evolution are determined by the quantitative analysis model of water-sediment interaction in the simulation of bedrock rivers. In this case, both hydraulic and bedrock-river hydraulic erosion conditions should be met. When the flow states are spatially consistent and the resistance factors (i.e. ρ, C_f, and g in Equation 8) are constant, we can uniquely determine k_q and k_w from Equations 6 and

9, respectively, and the coefficient K from Equation 10-1 is a constant. Second, the river should be in equilibrium to eliminate the erosion response lag. Although the DS model does not have an erosion coefficient K, if the aforementioned resistance factors are uniformly classified in the independent variable R in Equation 2, then R will be the sum of the lithologic and the rock-flow antagonist resistances; that is, Equation 2 is equivalent to Equation 9. Similarly, the law of the conservation of matter can also be introduced into the DS model:

$$dz / dt = U - I_{grade} \quad (14)$$

Hence, both the DS and AS models can be used to quantitatively analyze the relationship between river incision and rock uplift.

3. MATERIALS AND METHODS

3.1. Overview of the Gyirong Watershed

The Gyirong Watershed (85°10′–85°40′E, 28°15′–28°45′N, area of 2,108.59 km^2) is located in the upper reaches of the central section of the Ganges River on the west side of Mount Shishapangma. The main stream of the Gyirong Zangbo River originates in the southern foothills of Dajila Mountain. After passing Resuo Bridge Port, the river is known as the Te'ersurli River, which flows into the Gandak River in front of the Himalayas in Nepal and merges with the Ganges River near Patna, India. The basin runs approximately perpendicular to the Himalayan ridge. The divide is high in the north and low in the south and contains steep fault blocks. The areas at altitudes greater than 6,000 m are covered by glaciers.

According to the local structural geology, lithology, and landscape, the Gyirong Watershed can be divided into 3 units (Fig. 2): ① The Tibetan Himalayan unit is located in the upper reaches of the watershed. This unit is a wide alluvial valley covering most of the Gyirong Basin. The geological substrata are the Tethys-Himalaya sedimentary fold-and-thrust belt. The hanging wall of the Boerjielajia-Qiongga reverse fault is composed of Jurassic-Cretaceous shallow marine clasolite, carbonatite, and siliceous rocks sedimentary formations, while the footwall consists of Sinian-Jurassic marine clasolite and carbonatite (Zhang, 2003; Zhang et al., 2006). ② The Southern Tibet Detachment Structure (STDS) unit is the valley located in the middle reaches of the watershed, and its terrain is deeply constrained by the STDS shear tectonic forces. From Woma Village, the SSW Gyirong Zangbo River crosses 6 sets of near-EW normal and reverse faults, and then, it enters an area containing ancient metamorphic Himalayan crystalline rocks. As the valley becomes narrower and the river gradient increases, numerous rock outcrops are exposed in the riverbed and on the riverbank. ③ The higher Himalayan unit is located in the downstream canyon, south of Zhuotang Village, where the Sinian metamorphic rocks were created by the intrusion of Miocene granites (Zhang, 2003). The river gradient is higher where the river is narrow and deep, and the riverbed and riverbank are strongly scoured. A 10-km-long glacial erosive valley extends throughout Maga Village, Bangxing Village and Gyirong Town. Debris flow deposits now fill the valley, which used to be a barrier lake (Wang, 2011).

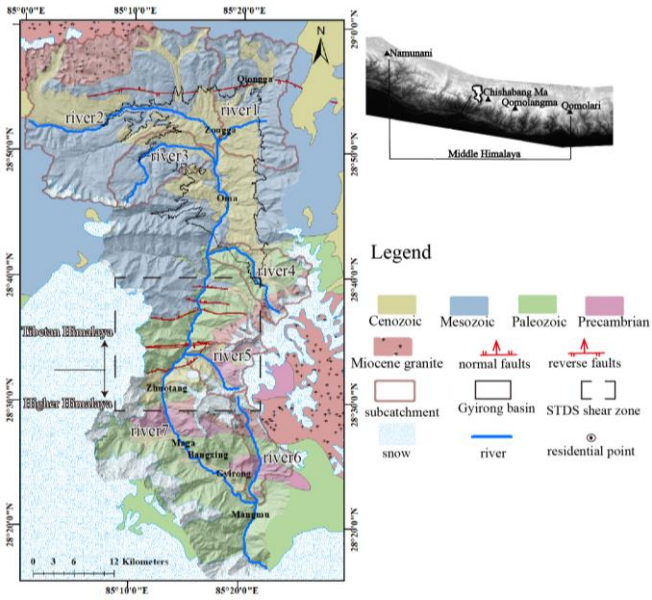

Figure 2 Geological and geomorphic map of Gyirong Watershed

3.2. Data Source

The ASTER GDEM 2 file of the study area was obtained, with WGS 1984 as the plain datum and EGM 96 as the height datum. At a confidence level of 95%, the overall precision of the data is about 17 m and the horizontal precision is about 75 m. The file was projected onto a UTM map at 45°N in ArcGIS. In addition, a 1:250000 geologic map of Gyirong County (China Geological Survey, 2003) and a 1:250000 vector geographic feature data set of the Everest Nature Reserve were also used. Both of these maps were consistent with the projection of the Aster GDEM file.

3.3. Methods

3.3.1 Selection of rivers and smoothing of river profiles

We used ArcGIS 10.2 to calculate the flow direction, flow acceleration, and river network extent from the raster datasets using the Deterministic 8

(D8) method (O'Callaghan & Mark, 1984). Then, we classified the river network using Strahlter's method (Strahler, 1953). Prior to our analyses, we had to make two specific adjustments: first, we wanted to determine the position of headwater using digital elevation models (DEM). Bisson et al., (2017) proposed that the formation condition of runoff is the drainage area is greater than 1 km^2 (Montgomery & Foufoula-Georgiou, 1993). In this study, we used a flow acceleration greater 1000 pixels (i.e. a contributing area of 0.9 km^2) as the minimum pixel value. Second, we adjusted the original GDEM via pit-filling to account for empty data values. With these adjustments, we were able to easily select the rivers and smooth the river profiles.

When it came to selecting rivers, we picked rivers with similar tectonic histories and classifications. The Gyirong Watershed contains 74 sub-watersheds and 5 levels of tributaries; however, only 6 sub-watershed areas contain level 4 tributaries (Fig. 2a-f). By overlaying the GDEM onto the 1:250000 geologic map, we were able to trace the river sources back from the mouths of the 6 sub-watersheds to extract 6 complete level-4 water channel masks (Fig. 2). The river's elevation was then extracted to calculate topographic indicators such as the gradient, upstream drainage area, and the upstream distance.

Our next step was to smooth the river profiles. Due to the quality of the DEM after applying the pit-filling algorithm, the original river profiles are often characterized by sudden jumps or obvious steps (Fig. 3) (Harbor et al., 2005), which must be smoothed. A variety of smoothing methods have been proposed (Harbor et al., 2005; Montgomery & López-Blanco, 2003; Snyder et al., 2000). In this study, the spatial resolution of the GDEM is the same as the USGS map (30 m) shown in Snyder's (2000) study of the Mendocino triple junction region in northern California. We then applied Snyder's 10 m interval least squares method to smooth the river's longitudinal profile, a technique that is analogous to sampling elevations in 10 m intervals from topographic maps. Then, the gradient, upstream distance, and drainage area corresponding to the altitude intervals were sequentially smoothed (the calculation results see S1 in Data Repository). Although this method cannot increase the resolution of the DEM, each original elevation value can be fully utilized.

3.3.2. Fitting of the river profiles

To reduce the fitting error, we applied a regression analysis to the river network classifications and fit each river according to four regression lines (Fig. 4). Then, we plotted the distribution histogram of fit errors(*r)* and calculated the confidence interval P corresponding to the 95% confidence level as an index to evaluate the models (Fig. 5). The smaller the P value, the more concentrated the *r* between the fitted gradient and the actual gradient became, and thus, the better the model's fitting performance became.

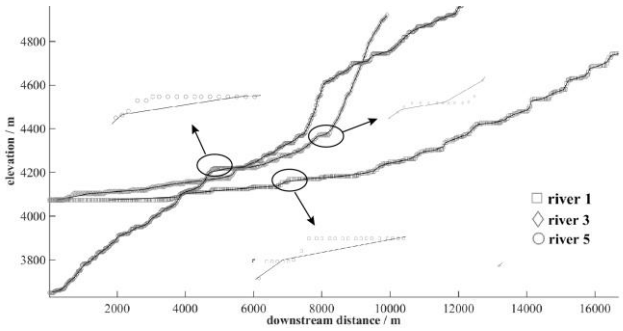

Figure 3 profiles comparation between the raw DEM extracted and the smoothed. Rivers 1, 3 and 5 are located at Tibet Himalaya and Higher Himalaya separately. on the raw DEM, the phenomenon of sudden jumps and steps is more obvious regardless of the geological settings.

3.3.3. Identification of knickpoints

The knickpoints were visually interpreted from the scatter diagrams of both models plotted using the same coordinate system (Fig. 6). The Gyirong Zangbo River is the highest classification channel (Fig. 2). We also conducted a knickpoint identification analysis.

4. RESULTS

4.1. Fitting Error

As shown in figure 5, the fitting errors of the two models are normally distributed. The values of r_{River1} and r_{River6} ranged from −2.5 to 2 and were concentrated in the ±0.5 interval. The range of the r_{River7} values was slightly larger, i.e., −5.5 to 3. Although it has obviously been shifted to the right, like the other rivers, it still has a single peak, aggregating at ±1. By comparing the confidence interval P at a confidence level of 0.95, we found that $P_{AS}<P_{DS}$ from River 1 to River 4, indicating that the AS model outperforms the DS model in this area. However, $P_{AS}>P_{DS}$ from River 5 to River 6, indicating that the DS model is superior to the AS model in this area. The confidence interval of river 7 has the largest span, and $P_{AS}>P_{DS}$. Since the river is more than 86 km long, the DS model outperforms the AS model in simulating long river channels.

4.2. Identification of Knickpoints

The knickpoints were divided into 4 types based on the scatter plot (Fig. 6). ①. The data points

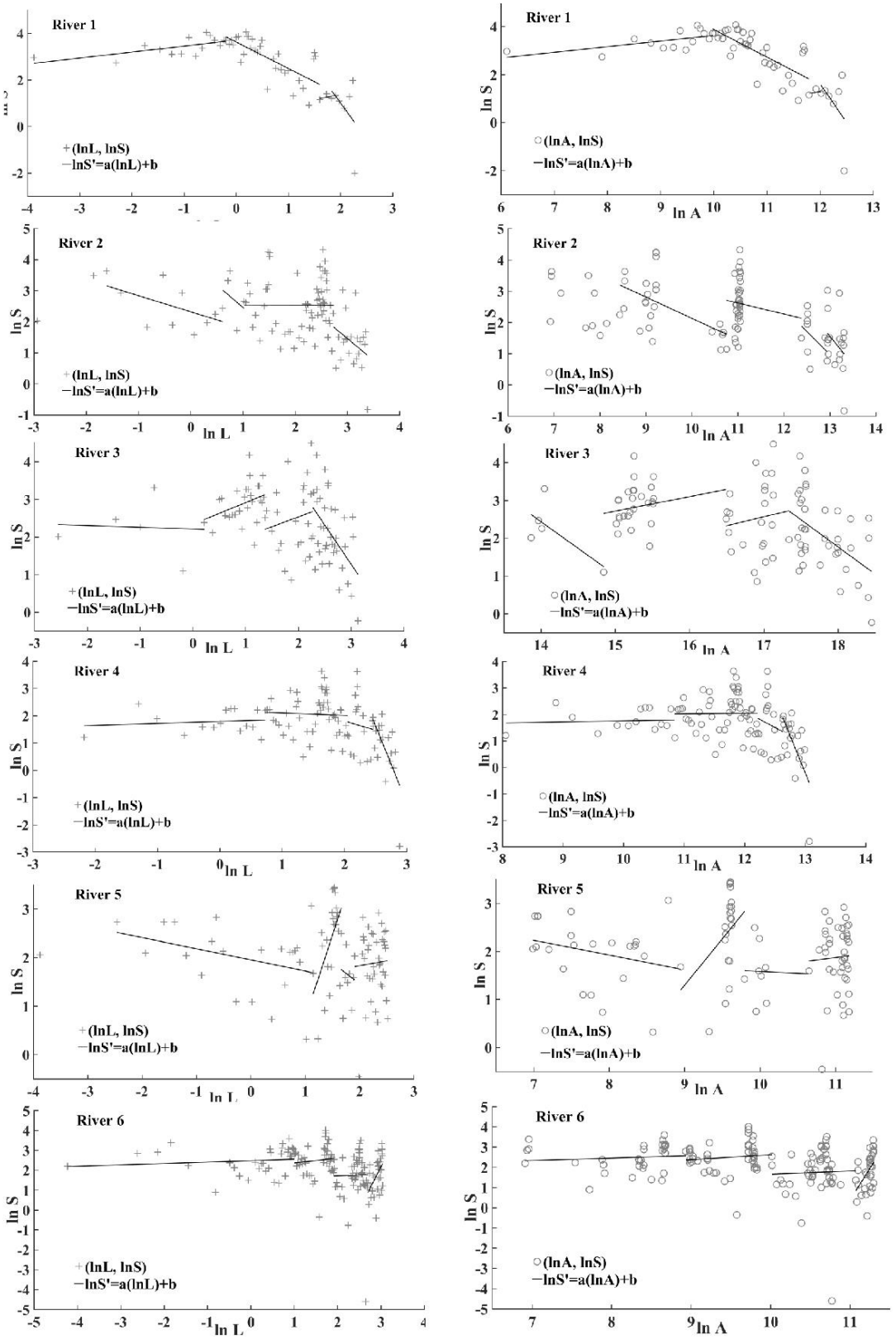

Figure 4 Fitting of river 1-6 profiles. DS model fitted is left and AS model right used equations 3 and 11 separately. *lnS'* is the fitting value. River 7 is the fifth channel, so the cracked sections fitting method is adopted (Fig. 9). *a* and *b* are the regression coefficients (results are in S2 in Data Repository).

are regular and the knickpoints are clear (e.g. River 1). ②. The data points do not correlate with the upstream distance or the drainage area. As can be seen from Figures 1B and 1C; for Rivers 2, 3, and 4, only the relatively large gradient values can be identified as the potential knickpoints. ③. Similar to

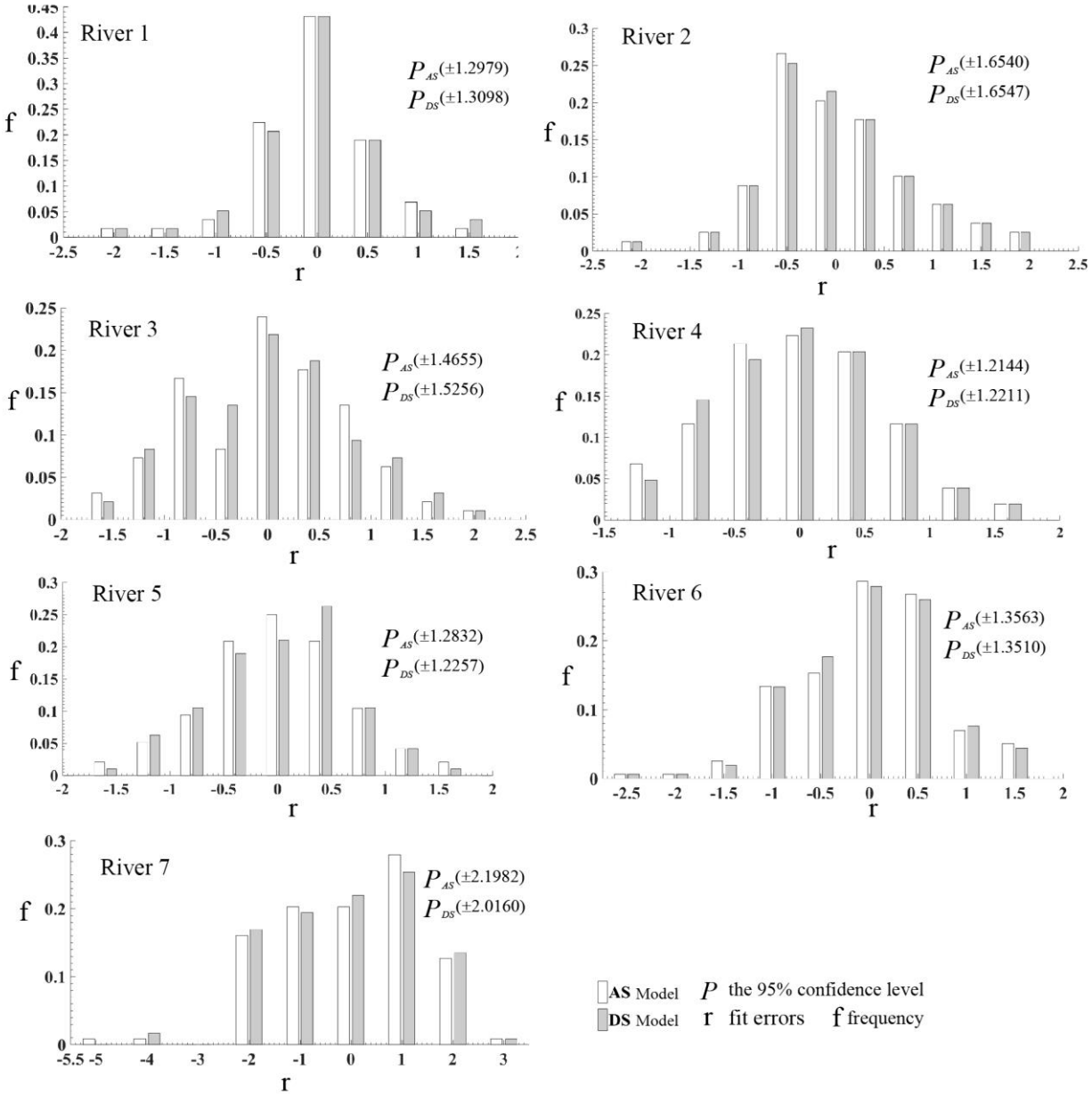

Figure 5 the error histogram of lnS' minus lnS. r is the error; f is the frequency of r and P is the confidence interval for 95%. The white bar is plotted by AS model and the gray bar is by DS model.

Figure 1B, the data points on the scatter plot are clearly segmented or abruptly vertically change, and the knickpoints are easily identifiable on the AS plot (e.g. Rivers 5 and 6). ④. The data points are distributed similarly to the type ③ data points, but the knickpoints are easily identifiable on the DS model (e.g. River 7)

We observed a total of 45 knickpoints along the 7 rivers (Fig. 7, see S3 in Data Repository for the attributes of these knickpoints), three of which have elevations higher than 5050 m (Rivers 3 and 4; Fig. 3). This elevation is indicative of a periglacial zone, where the knickpoints are affected by seasonal freezing and thawing; for this reason, they are usually excluded from analyses of tectonogeomorphic evolution. Thirty-two of the total knickpoints have elevations between 3950–5050 m. The last 10 knickpoints, which are located in the middle and lower reaches of Rivers 5, 6, and 7, have elevations lower than 3950 m (Fig. 3). Excluding the 3 in the periglacial zone, the gradient of the other 37 knickpoints is less than 75°, which is the dominant slope interval. With a gradient lower than 25° as the critical value of a stable hillside (Kühni & Pfiffner, 2001), we divided these knickpoints into the following 3 classifications: stable (gradient less than 25°), unstable (gradient greater than 25° but less than 75°), and extremely unstable (gradient higher than 75°). Ten of the knickpoints were stable, 24 were unstable, and 8 were extremely unstable. The majority of the knickpoints with elevations of 3950–5050 m was either stable or unstable.

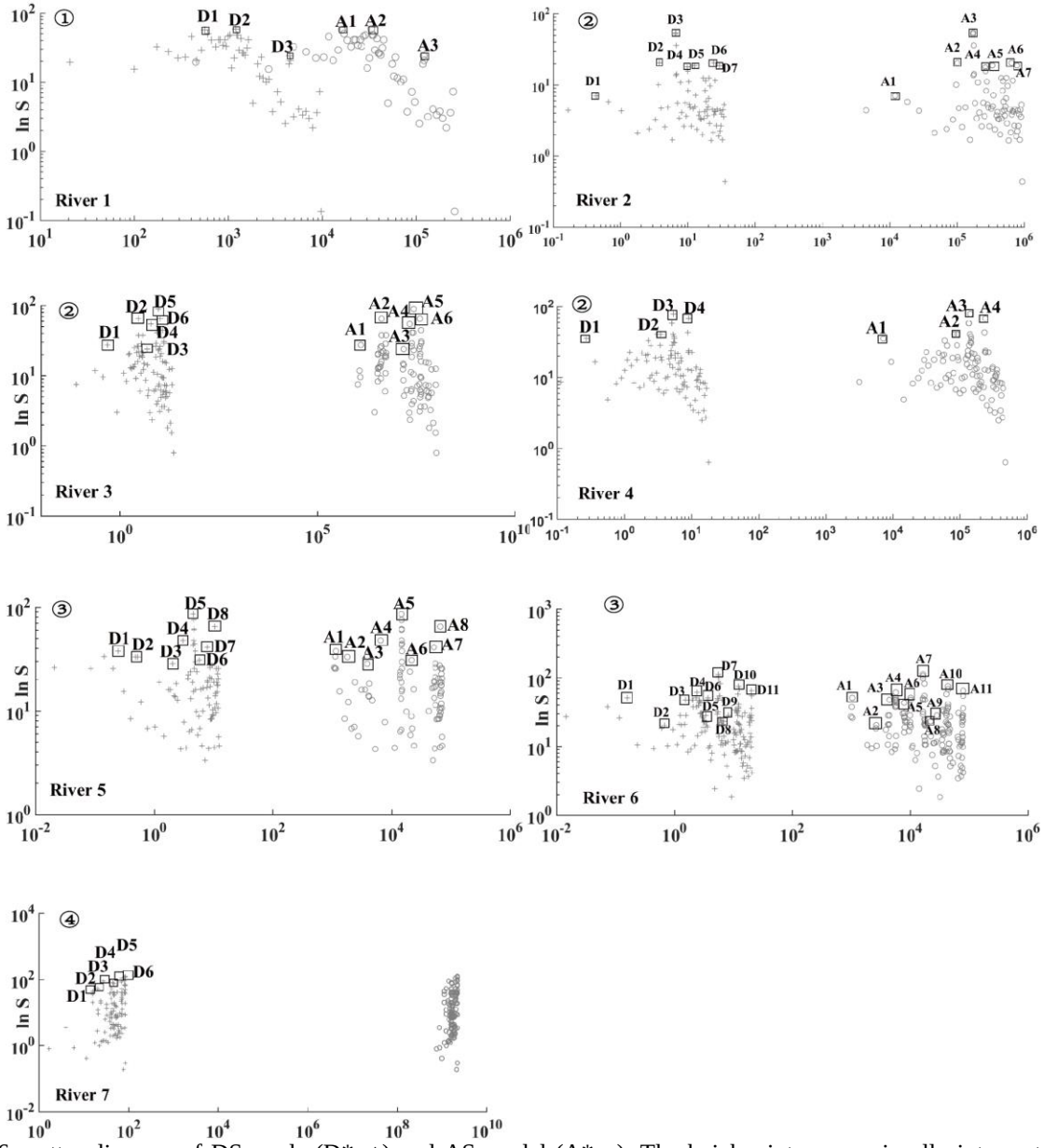

Figure 6 scatter diagram of DS mode (D*, +) and AS model (A*,). The knickpoints were visually interpreted from Figure 1. If there are obvious A and B channel segments, the knickpoints°can be identified. If there is no obvious segmentation, i.e., with the maximum gradient of the local area acting as a potential knickpoint. This study focused on the identification of knickpoints, so potential knickpoints were also noted. Artificial knickpoints such as reservoirs and dams were excluded based on a field survey. Currently, no hydroelectric engineering is located in the 6 sub-watersheds.

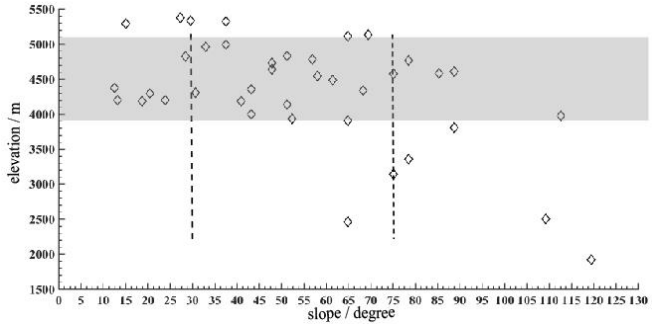

Figure 7 Relationship between the slope and the elevation of 45 knickpoints. The gray strip covers a range of 3950m to 5050m. The dotted lines point to stable gradient (25°) and extreme unstable gradient (75°)

5. DISCUSSION

5.1. Comparison of Model Results

Both the AS and DS models are characterized by power functions, but their independent variables differ. Their dependent variables are identical, but their independent variables significantly differ from each other when defining the domain and the value of the upstream distance is much smaller than that of the drainage area. If the performance of the models is based on the functional relationship and the value of the variables, then the results should contain regular systematic errors. However, according to the fitting

results, the AS model outperforms the DS model for Rivers 1–4, while the DS model outperforms the AS model for River 5–7. As for the interpretation of the knickpoints, the two models have the same performance for Rivers 1–4, the AS model performs slightly better than the DS model for Rivers 5–6, and the DS model performs slightly better than the AS model for River 7. Obviously, this result is irregular, indicating that the suitability of the model is not determined by the structure of the model. Therefore, the degree to which the river state matches the conditions for applying the model may be more critical. For the Gyirong Watershed, the degree to which the river meets or deviates from equilibrium seems to be of great significance.

Rivers 1–6 can be divided into 2 types based on their tectonogeomorphic units, lithology, and climate. The erosion datum of Rivers 1–4 is about 4000 m, the river altitude difference is small, the bedrock is composed of Tibetan Himalayan sedimentary rocks, and the climate is cold and prone to droughts. Rivers 5–6 have an erosion datum of less than 2000 m, the altitude difference is large, the bedrock is composed of Higher Himalayan crystalline rocks, and the climate changes from wet to cold and drought prone with increasing elevation. During structural uplift and downward erosion, the hydraulic effect acting on Rivers 5–6 should be more severe than that on Rivers 1–4. In other words, Rivers 1–4 are more balanced than Rivers 5–6. As was previously mentioned, the AS model has stricter equilibrium requirements. Therefore, the AS model simulates Rivers 1–4 better and is more sensitive to changes in the knickpoints of the unbalanced Rivers 5–6. However, River 7 is an exception. The DS model outperforms the AS model in both river simulation and interpretation of the knickpoints. Whipple (2004) suggested that the AS model is applicable to rivers in equilibrium with an average length of 3–50 km, while other researchers proposed that the DS model is better suited for long rivers (Goldrick & Bishop, 2007). According to the comparison conducted in this study, the DS model performs better for disequilibrium long rivers.

5.2. Spatial Distribution Characteristics of the Knickpoints

The knickpoints exhibit significant spatial variation, and their classification is strongly influenced by their structural intensity. The areas with elevations of 3950–5050 m include the Tibetan Himalayas (including the STDS) and the area above the Gyirong Valley in the Higher Himalayas. In the areas with elevations of less than 3950 m, the terrain gradually gentles, forming the deep Gyirong Valley (Fig. 8). The stable knickpoints are concentrated in the Tibetan Himalayas, which have less relief. The 8 stable knickpoints on rivers 1–3 account for 4/5 of the total number of stable knickpoints. In contrast, the unstable knickpoints are densely distributed at the intersections of rivers and in major faults and folds where tectonic deformation is quite intense, e.g., the upper plate of the Eastern Oma normal fault (R1a, R1b) and the axis of the Gongdang-Gunda anticline (R4a, R4c). In particular, there are 10 unstable knickpoints on rivers 5–6 on the lower plate of the Langgele normal fault. In addition, the extremely unstable knickpoints are concentrated in the area where the Gyirong Valley segment of River 7 intersects EW-trending normal and reverse faults.

It has been reported that climate also affects the spatial distribution of knickpoints. In particular, knickpoints are often found in areas of retrogressive erosion in rivers with abundant rainfall and strong surface runoff (Struth et al., 2019; Ahmed et al., 2018; Gonga-Saholiariliva et al., 2011). To some extent, the knickpoints identified in this study are related to the modern climate of the Gyirong Watershed. The stable knickpoints are primarily located at elevations of more than 4000 m where the annual precipitation is less than 300 mm (Yang, 2011) and seasonal glacial meltwater and weathering are the main causes of erosion. A large number of extremely unstable knickpoints are located in the Gyirong Valley where the annual precipitation is greater than 1000 mm (Yang, 2011), the terrain undulates significantly, and erosion is significantly stronger than at an elevation of 4000 m. However, the distribution of the knickpoints is not necessarily determined by the different climate patterns. As a matter of fact, the geomorphology at elevations of 2000 m to 7000 m in the Gyirong Watershed did not developed until the Late Pleistocene. The climatic differences are determined by the timing of the uplift and the corresponding elevation change in the mountain. To analyze the influence of climate on the geomorphic evolution of the Gyirong Watershed, it was necessary to explore the relationship between the structural uplift and the erosion rate. As the highest-level river channel in the Gyirong Watershed, the Gyirong Zangbo River (River 7) not only has the highest kinetic energy, but is the also most intensely eroded, making it the area experiencing the most geomorphic evolution. Since the DS model is more suitable for simulating long disequilibrium rivers, the characteristics of the parameters k and λ of River 7 were analyzed based on the DS model and the uplift and erosion process in the Gyirong Watershed were explored according to the tectonic evolution of this region.

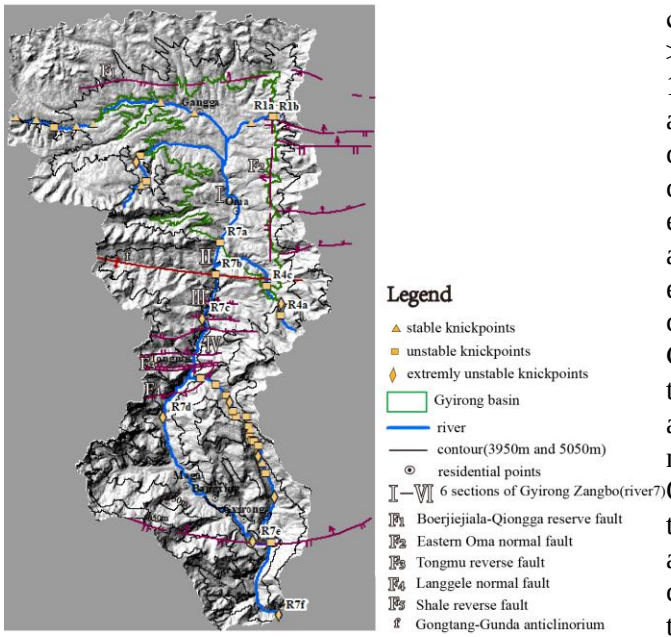

Figure 8 The relationship between tectonic, terrain and spatial distribution of the knickpoints

5.3. Profile Characteristics and Geomorphic Evolution of the Gyirong Zangbo River

Based on its source and the location of its knickpoints, River 7 can be divided into 6 sections, excluding the 3 km section from R7f to the estuary (Fig. 9). Sections I–II are located in the Tibetan Himalayan unit, sections III–IV are in the STDS unit, and sections V–VI are in the Higher Himalayan unit. The results presented in table 2 can be explained by the mathematical and physical meanings of the DS model. The small change in λ corresponds to a large change in k, i.e., a small change in the degree of convex-concaveness of the river will result in a significant change in the erosion rate. As can be seen from Figures 8 and 9, for channel segments I, IV, and VI, k≈0 and λ<0, indicating a small average erosion rate and a concave shape. Channel segments II, III, and V have k > 0. In channel segment II, k reaches a magnitude of 10^4 and λ>2, indicating a large average erosion rate and a very concave river channel. This phenomenon is consistent with Mode 2 in table 1, in which R is constant, indicating that the lithology is the same in each channel segment, while the average erosion rate along the length of the river is not in equilibrium. The erosion rate can be rapid or slow, and the concave and convex river channels are alternately distributed. Channel segments II and III are a typical reflection of this. The channel segments have a length of 11.7 km and an elevation of 3806–3996 m. Although rainfall is not abundant, the river has cut through the Gongdang-Gunda anticline and has reached the southern end of the Gyirong Basin (Fig. 8), indicating a strong erosion ability. Nevertheless, modern precipitation characteristics cannot explain this phenomenon, and the relationship between Himalayan uplift history and climate should be taken into consideration.

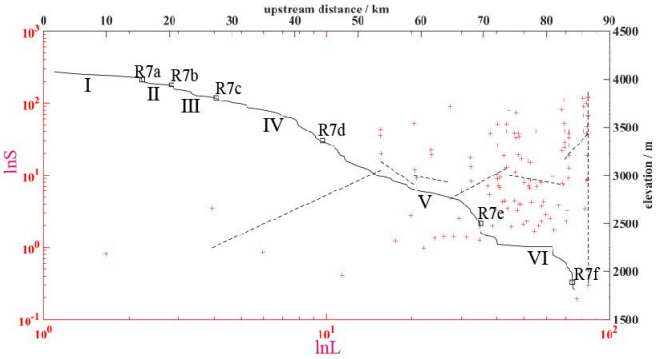

Figure 9 Longitudinal profile of Gyirong Zangbo river based on DS model. The river is 84.2km long, and it is almost perpendicular to all of the main tectonic blocks in the watershed. 6 knickpoints identified divide the river into 7 cracked sections. The fitting error(r) and confidence interval(P) are showed in figure 5

Table 2 the parameters of the cracked section of river 7

Knickpoint	Elevation (m)	Gradient (°)	Distance (km)	Channel segment	K*	λ*
R7-0†	4073					
R7a	3996	43.24	15.59	I	0.08	−1.80
R7b	3933	52.35	20.39	II	25375.34	2.70
R7c	3806	88.76	27.29	III	86.28	0.72
R7d	3356	78.52	44.21	IV	0.00	−2.13
R7e	2503	109.24	69.37	V	129.80	0.68
R7f	1884	122.90	84.20	VI	0.00	−4.15

† *R7-0 is the starting point of Gyirong Zangbo river.*

In contrast to the strong collisional orogeny during the Himalayan movement, the tectonic activity during the Qinghai-Tibet movement was dominated by deplanation and multi-phase uplift (China Geological Survey, 2003). This is supported by the existence of 7 terraces and one mountaintop erosion surface in the western part of the Gyirong Basin, which have an uplifted height of about 970 m (Zhu, 1995). Within about 200 ka, the Gyirong Zangbo River captured the Gyirong lake basin from the mountain divide due to strong erosion and continuous uplift. In the middle period (about 0.8 Ma) of the Kunlun-Huanghe Movement (1.2 Ma–0.6 Ma), most of the mountains reached an elevation of 4000–4500 m, placing them in the cryosphere. The Qinghai-Tibet Plateau has entered its maximum glacial period since the Quaternary (Wang et al., 1996a; Wang et al., 1996b). The upper reaches of the Gyirong Zangbo River also entered extremely cold elevations of more than 4000 m, resulting in the current climate pattern. The erosive force of the upstream channel segment gradually weakened, retaining traces of the retrogressive erosion that occurred in the previous period.

The erosion rate and degree of concaveness of channel segments I, IV, and VI decreased because of the influence of the fractures on the channel segments. Channel segment I was already a sedimentary area in the Gyirong Lake Basin period. Channel segment IV traversed the Tongmu reverse fault and the Langgele normal fault in the STDS unit (Fig. 9), blocking the products of the strong erosion transported by channel segments II and III and the tributaries. About 10 km of flat river in channel segment VI was located below the Shale reverse fault, providing space for the sediment carried by channel segment V. Due to the stronger glacial action during the Kunlun-Huanghe movement, the spatial relationship between river erosion and sedimentation became fixed. Hence, the profile of the Gyirong Zangbo River not only records information about the development of vertical variations in climate in the mountain hinterland as the Himalayas were uplifted over the past 2 Ma, it also reflects the spatial pattern of the interaction between river erosion and sedimentation in the same period.

6. CONCLUSIONS

Based on the applicability of the bedrock channel erosion model, the AS and DS models have different numerical responses to rivers with different levels of equilibrium. For river simulations, the AS model has a smaller error in simulating water channels in equilibrium, while the DS model fits disequilibrium river channels better. When it comes to the interpretation of knickpoints, there is no difference between the two models when simulating river channels in equilibrium, but as the disequilibrium of the river increases, the DS model is comparatively better. Our comparative analysis demonstrates that the two models have their own advantages and disadvantages. The rivers should be carefully selected and the equilibrium state of the rivers should be determined before applying the models. The geotectonic background of the region can provide effective prior knowledge for river prediction.

The geomorphic evolution of bedrock rivers is mainly controlled by the interaction between the structure, lithology, and climate. For the Himalayan orogenic belt, the timing and elevation of the uplift also needs to be considered. This study clearly demonstrates the variation in the erosion rate of a river in disequilibrium (the Gyirong Zangbo River) and the alternate distribution of concave and convex river channels. Such a feature cannot be directly explained by the geomorphic evolution factors. However, by analyzing the timing and elevation of the Himalayan uplift, the contradictions in the river erosion rate and the degree of concaveness in the alpine climate region were reconciled and the tectonic evolution of the river was investigated.

Since the AS and DS models have the same structure, if the AS model is used to calculate the parameters of the profile of the cracked section of river 7, similar numerical results can be obtained. Nevertheless, the AS model involves strict preconditions, i.e., with the equilibrium state of the bedrock channels. Even if the parameters of the AS model are calculated, it is difficult to formulate a reasonable explanation. However, although the DS model is more suitable for analyzing disequilibrium river channels, it is currently only possible to use the erosion rate and the degree of concaveness to make a semi-quantitative comparison of size or speed. On the contrary, due to the addition of temporal and spatial variables, the AS model's ability to quantitatively calculate the erosion rate and the uplift height has significantly improved (Perron & Royden, 2013; Whipple et al., 2017). In this study, the law of the conservation of matter was incorporated into the theoretical basis of the DS model and a differential equation containing the height z, time t, river uplift U, and average erosion rate I_{grade} (Equation 14) was designed. Further modification of the differential algorithm of the DS model based on the AS model, may be a new direction for the quantitative analysis of the geomorphic evolution of disequilibrium bedrock rivers.

Acknowledgements

This work was financially supported by the NNSFC (1461029), Natural Science Foundation of Tibet Autonomous Region (2015ZR-13-66) and the Project of Talent Introduction by Chengdu Normal University (YJRC2016-6). Thanks to the research materials from International Science & Technology Cooperation Program of China(2013DFR90670) and Innovation team of Sichuan Provincial Department of Education(14TD0039)

REFERENCES

Ahmed, M.F., Rogers, J.D. & Ismail, E.H., 2018. *Knickpoints along the upper Indus River, Pakistan: an exploratory survey of geomorphic processes.* Swiss Journal of Geosciences 111(1-2), 191-204.

Anderson, R., Hancock, G. & Whipple, K., 2015. *River incision into bedrock: Mechanics and relative efficacy of plucking, abrasion, and cavitation.* Geological Society of America Bulletin 112(3), 490-503.

Bishop, P. & Goldrick, G., 2000. *Geomorphological evolution of the East Australian continental margin*. In: S.M. A (S.M. A), Geomorphology and Glocal Tectonics. Wiley, Chichester, pp. 227-255.

Bisson, P.A., Montgomery, D.R. & Buffington, J.M., 2017. *Chapter 2 – Valley Segments, Stream Reaches, and Channel UnitsMethods in Stream Ecology*, Volume 1 (Third Edition), pp. 21-47.

Brookfield, M.E., 1998. *The evolution of the great river systems of southern Asia during the Cenozoic India-Asia collision: rivers draining southwards*. Geomorphology 22(3-4), 285-312.

Brookfield, M.E., 2008. *Evolution of the great river systems of southern Asia during the Cenozoic India–Asia collision: Rivers draining north from the Pamir syntaxis*. Geomorphology 100(3-4), 296-311.

China Geological Survey., 2003. Regional geological survey report of Gyirong Basin (1:250000).

Flint, J.J., 1973. *Stream gradient as a function of order, magnitude, and discharge*. Water Resources Research 10(5), 969-973.

Formento-Trigilio, M.L. & Pazzaglia, F.J., 1998. *Tectonic geomorphology of the Sierra Nacimiento: traditional and new techniques in assessing long-term landscape evolution in the southern Rocky Mountains.* Journal of Geology (106), 433-453.

Goldrick, G. & Bishop, P., 2007. *Regional analysis of bedrock stream long profiles: evaluation of Hack's SL form, and formulation and assessment of an alternative (the DS form).* Earth Surface Processes and Landforms 32(5), 649-671.

Gonga-Saholiariliva, N., Gunnell, Y., Harbor, D. & Mering, C., 2011. *An automated method for producing synoptic regional maps of river gradient variation: Procedure, accuracy tests, and comparison with other knickpoint mapping methods.* Geomorphology 134(3-4), 394-407.

Hack, J., 1973. *Stream-profile analysis and stream-gradient index.* Bulletin of the American Astronomical Society 25(1), 421-429.

Hack, J.T., 1957. *Studies of Longitudinal Stream Profiles in Virginia and Maryland.* Geological Survey Professional Paper 294, 45-97.

Harbor, D., Bacastow, A., Heath, A. & Rogers, J., 2005. *Capturing Variable Knickpoint Retreat in the Central Appalachians, USA.* Geomorphology 28(9), 23-36.

Howard, A.D., Dietrich, W.E. & Seidl, M.A., 1994. *Modeling fluvial erosion on regional to continental scales.* Journal of Geophysical Research-Solid Earth 99(B7), 13971-13986.

Howard, A.D. & Kerby, G., 1983. *Channel changes in badlands.* Geological Society of America Bulletin 94(6), 739-752.

Kirby, E., Whipple, K.X., Tang, W. & Chen, Z., 2003. *Distribution of active rock uplift along the eastern margin of the Tibetan Plateau: inferences from bedrock channel longitudinal long profiles.* Journal of Geophysical research 108, 2217.

Kühni, A. & Pfiffner, O.A., 2001. *The relief of the Swiss Alps and adjacent areas and its relation to lithology and structure: topographic analysis from a 250-m DEM.* Geomorphology 41(4), 285 - 307.

Montgomery, D.R. & Foufoula-Georgiou, E., 1993. *Channel Network Source Representation Using Digital Elevation Models.* Water Resources Research 29(12), 3925-3934.

Montgomery, D.R. & López-Blanco, J., 2003. Post-Oligocene river incision, southern Sierra Madre Occidental, Mexico. Geomorphology 55(1-4), 235-47.

O'Callaghan, J.F. & Mark, D.M., 1984. *The extraction of drainage networks from digital elevation data.* Computer Vision Graphics & Image Processing 28, 323-344.

Perron, J.T. & Royden, L., 2013. *An integral approach to bedrock river profile analysis.* Earth Surface Processes and Landforms 38(6), 570-576.

Seever, L. & Gornitz, V., 1983. *River profiles along the Himalayan Arc as indicators of active tectonics.* Tectonophysics 92(4), 335-367.

Snyder, N.P., Whipple, K.X., Tucker, G.E. & Merritts, D.J., 2000. *Landscape response to tectonic forcing: Digital elevation model analysis of stream profiles in the Mendocino triple junction region, northern California.* Geological Society of America Bulletin 112(8), 1250-1263.

Strahler, A.N., 1953. *Hypsometric (area-altitude) analysis of erosional topography.* Geological Society of America Bulletin 63(11), 1117-1142.

Struth, L., Garcia-Castellanos, D., Viaplana-Muzas, M. & Vergés, J., 2019. *Drainage network dynamics and knickpoint evolution in the Ebro and Duero basins: From endorheism to exorheism.* Geomorphology 327, 554-571.

Vijith, H., Prasannakumar, V., Sharath Mohan, M.A., Ninu Krishnan M.V. & Pratheesh, P., 2017. *River and basin morphometric indexes to detect tectonic activity a case study of selected river*

basins in the south Indian Granulite Terrain (SIGT). Physical Geography 38(4), 360-378.

Wang F.B., Li, S.F., Zhang, J., Yan, G., 1996a. *The Formation and evolution of Gyirong Basin, environmental change and Himalayan uplift.* Science China: Earth Sciences (Series D) 26(4), 329-335.

Wang, D.C., Zhang, J.J., Yang, X.Y., Qi, G.W., 1996b. *Tectonic and environmental evolution of Gyirong Basin, and its relationship to the uplift of Tibetan Plateau.* Acta Scientiarum Naturalium Universitatis Pekinensis 45(1), 79-89.

Wang, J., 2011. *Study on the quality of geological environment of Gyirong Basin.* Chengdu University of Technology. pp.11.

Whipple, K.X., 2004. *Bedrock Rivers and The Geomorphology of Active Orogens.* Annual Review of Earth and Planetary Sciences 32(1), 151-185.

Whipple, K.X., DiBiase, R.A. & Crosby, B.T., 2013. *Bedrock Rivers.* In: J. Shroder and E. Wohl (J. Shroder and E. Wohl (Editors), Treatise on Geomorphology. Academic Press, San Diego, CA, Fluvial Geomorphology, pp. 550-573.

Whipple, K.X., Forte, A.M., DiBiase, R.A., Gasparini, N.M. & Ouimet, W.B., 2017. *Timescales of landscape response to divide migration and drainage capture: Implications for the role of divide mobility in landscape evolution.* Journal of Geophysical Research: Earth Surface 122(1), 248-273.

Willgoose, G., 1994. *A physical explanation for an observed area-slope-elevation relationship for catchments with declining relief.* Water Resources Research 30(2), 151-159.

Yang, R.F., 2011. *Study on the Chongzhui accumulation body's cause of formation of Gyirong Basin.* Chengdu University of Technology. pp.11.

Zhang, Z.L., 2003. *Regional geological survey report of Gyirong of the People's Republic of China.* China Geological Survey.

Zhang, Z.L., Sun, X., Li, G.D, Zhang J.D., Liu H.Z., Zhuan S.P. & Wei W.T., 2006. *New explanation of detachment structures in the Burang and Gyironggou regions, southern Xizang.* Sedimentary Geology and Tethyan Geology 26(2), 1-6.

Zhu, C., 1995. *Neotectonism and quaternary glaciation of Gyirong basin, Xizang.* Mountain Research 13(4), 219-225.89.

Received at: 29. 05. 2020
Revised at: 03. 08. 2020
Accepted for publication at: 17. 08. 2020
Published online at: 26. 08. 2020